

# STRING RIBBON SILICON SOLAR CELLS WITH 17.8% EFFICIENCY

D.S. Kim, \*A.M. Gabor, V.Yelundur, A.D.Upadhyaya, V.Meemongkolkiat, A. Rohatgi  
University Center for Excellence in Photovoltaic Research and Education; School of Electrical and Computer Engineering,  
Georgia Institute of Technology, Atlanta, GA 30332 USA  
\*Evergreen Solar Inc., 259 Cedar Hill St., Marlboro, MA 01752 USA

## ABSTRACT

We have fabricated 4 cm<sup>2</sup> cells on String Ribbon Si wafers with efficiencies of 17.8% using a combination of laboratory and industrial processes. These are the most efficient String Ribbon devices made to date, demonstrating the high quality of the processed silicon and the future potential for industrial String Ribbon cells. Cofiring PECVD (Plasma Enhanced Chemical Vapor Deposition) silicon nitride (SiN<sub>x</sub>) and Al was used to boost the minority carrier lifetime of bulk Si. Photolithography front contacts were used to achieve low shading losses and low contact resistance with a good blue response. The firing temperature and time were studied with respect to the trade-off between hydrogen retention and aluminum back surface field (Al-BSF) formation. Bulk defect hydrogenation and deep Al-BSF formation took place in a very short time (~1 sec) at temperatures higher than 740 °C.

## 1. INTRODUCTION

String Ribbon Si wafers are grown by a vertical sheet growth technique that is currently in multi-megawatt production at Evergreen Solar. This technique produces low cost Si due to the high utilization of the Si feedstock and the absence of ingot sawing and wafer etching.

The high quality of the processed String Ribbon wafers has been previously demonstrated [1] through high minority carrier lifetimes following cell processing. Recent research on processing String Ribbon cells has focused on industrial-type processing using screen-printing for metallization and the relatively deep junctions necessary for firing the screen printable inks and PECVD SiN<sub>x</sub> for defect passivation. A few years ago, a record high 16.2% efficiency cell was fabricated using photolithographic techniques [2]. However, recent cells made with screen-printing are now approaching the 16% level [3]. Therefore, we revisited laboratory cell production to demonstrate the even higher potential of this material.

One of the laboratory processing schemes we have implemented is rapid thermal processing (RTP) for simultaneous Al-BSF formation and passivation of bulk defects through hydrogenation from a SiN<sub>x</sub>:H layer. Here we push the RTP process toward shorter dwell times and lower temperatures than we have previously explored and examine the effects on the resulting Al-BSF quality and defect passivation.

## 2. BACKGROUND

The cell process employed by Georgia Tech in the past to produce the 16.2 % cell involved the following:

1. POCl<sub>3</sub> diffusion to form ~ 85 Ω/□ emitter and removal of diffusion glass in HF
2. Evaporation of Al and alloying at 850 °C
3. Evaporation of Al-Ti-Pd-Ag for back contact formation
4. Photolithography of the front contacts using evaporation of Ti-Pd-Ag and lift-off followed by Ag plating
5. Mesa etching for area definition
6. Forming gas annealing at 400 °C
7. Evaporation of ZnS/MgF<sub>2</sub> double AR coating

The recent process used by Georgia Tech for screen printing involves the following:

1. Belt furnace diffusion to form 40-50 Ω/□ emitter and removal of diffusion glass in HF
2. SiN<sub>x</sub> deposition on the front side
3. Screen printing of Al paste on the back followed by RTP or belt furnace annealing at 700-800°C
4. Screen printing of Ag paste for the front contact and RTP or belt furnace annealing

Phosphorus and Al gettering are common to both techniques and are known to contribute to improved minority carrier lifetimes. However, cofiring of SiN<sub>x</sub> and Al is a critical step for significant enhancement in bulk lifetime [4]. In this paper the high efficiency process has been modified to take advantage of this effect. The cofiring temperature and time were optimized to achieve maximum hydrogenation of defects.

## 3. EXPERIMENTAL

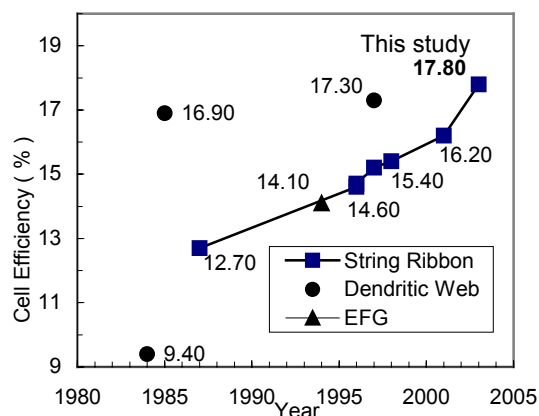
Standard String Ribbon wafers were pulled from the Evergreen production line with an average thickness of 300 μm and a resistivity of 3 Ωcm. P-type, 300 μm thick, 2 Ωcm FZ wafers were also used in this study. The String Ribbon silicon wafers were cut to an optimum size for tube diffusion and cleaned/etched in cleaning solutions of 2:1:1 H<sub>2</sub>O:H<sub>2</sub>O<sub>2</sub>:H<sub>2</sub>SO<sub>4</sub>, 15:5:2 HNO<sub>3</sub>: CH<sub>3</sub>COOH:HF, 2:1:1 H<sub>2</sub>O:H<sub>2</sub>O<sub>2</sub>:HCl. The phosphorus diffusion was performed at 870 °C for 32 minutes using a liquid POCl<sub>3</sub> source in a tube furnace to obtain an 85 Ω/□ n<sup>+</sup> emitter. The SiN<sub>x</sub> films were deposited by PECVD at Evergreen Solar on the phosphorus-diffused emitters. Aluminum paste (Ferro FX 53-038) was screen-printed on the back surface of the wafers. The SiN<sub>x</sub> on the front and the Al film on the rear were fired simultaneously in an RTP chamber to enhance hydrogen passivation. The ramp-up and cooling rates were set to >50 °C/sec for all the firing processes to achieve a uniform Al-BSF layer [5].

The firing temperatures were varied from 700 to 800 °C for 1 second and 60 seconds in order to study the

effects of firing temperature and time on the cell performance. The range of firing temperatures used in this study was determined from optimization of screen-printed String Ribbon solar cells, also being presented at this conference [6]. The processing temperature was measured by a thermocouple in physical contact with the front side of wafer. The front metal grid was defined by a photolithography process followed by removal of the  $\text{SiN}_x$  film in the grid region by etching in HF. Front contacts were formed by evaporating 60 nm Ti, 40 nm Pd and 60 nm Ag followed by a lift-off procedure. Additional Ag was plated to increase grid thickness and reduce series resistance. Nine  $4 \text{ cm}^2$  cells on each wafer were isolated using a dicing saw and then annealed in forming gas (4 % hydrogen in nitrogen) for 30 min. Emitter saturation current density ( $J_{0e}$ ) was measured by Sinton's PCD method. Optical properties of the  $\text{SiN}_x$  were characterized using a spectroscopic ellipsometer (J.A. Woollam Co., Inc.) to determine the optimal design of a double layer antireflection coating. In order to minimize reflectance, the  $\text{SiN}_x$  thickness was adjusted to 67.8 nm by etching the film in HF. Magnesium fluoride (99.5 nm) was coated on the  $\text{SiN}_x$  by vacuum evaporation to form a double antireflection coating layer. Long wavelength internal quantum efficiency (IQE) measurements were performed to characterize the Al-BSF of a finished solar cell. The thickness of the screen-printed aluminum was measured to be  $\sim 25 \mu\text{m}$  by profilometry (Alpha-Step 200) after drying the screen-printed Al. The thickness of the Al-BSF was measured by cross-section Scanning Electron Microscopy (SEM) after etching the heavily p-doped region selectively in 1:3:6 HF:HNO<sub>3</sub>:CH<sub>3</sub>COOH for 10 seconds [7]. In order to study just the quality of Al-BSF and its impact on the cell performance, photolithography cells were fabricated on FZ wafers with high quality rapid thermal oxide (RTO) on the emitter capped with ZnS/MgF<sub>2</sub> double layers.

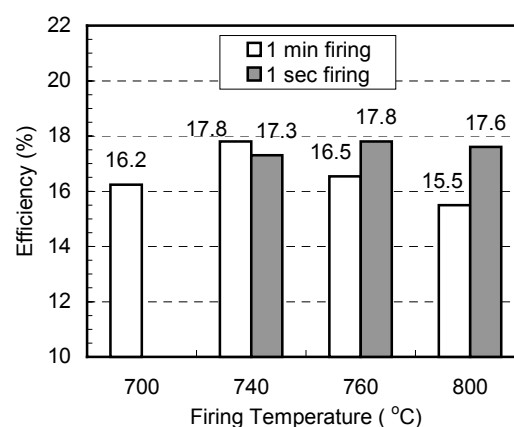
#### 4. RESULTS AND DISCUSSION

Fig.1 shows the progress in efficiency of ribbon solar cells with photolithography contacts. Data for Dendritic Web and EFG is limited. The best cells made in this study had NREL verified efficiencies of 17.8%, a new record for String Ribbon.



**Fig. 1** Progress in efficiency of laboratory scale ribbon solar cells.

Fig.2 shows the efficiencies of String Ribbon cells in this study as a function of firing temperature and time. The cell parameters are summarized in Table 1 with process parameters. A cell with 17.8 % efficiency was obtained at 740 °C for 60 second firing time. For a 60 second firing, the efficiency dependence on firing temperature was similar to that of fully screen-printed cells which showed maximum efficiency at 740 °C and rapid decrease in efficiency above 740 °C. However, the efficiencies for 1 second firing were found to be less sensitive to the firing temperatures, resulting in an equivalent maximum efficiency of 17.8 % at 760 °C. It is noteworthy that a very short one second firing gave the same efficiency as 60 seconds.



**Fig. 2** Efficiencies as a function of firing temperature and time for Al-BSF.

**Table 1.** Light I-V data for PL cells (masked to  $3.8 \text{ cm}^2$ ) fabricated on String Ribbon Si, measured by National Renewable Energy Laboratory.

Time (sec)	Temp (°C)	Eff. (%)	$V_{oc}$ (mV)	$J_{sc}$ ( $\text{mA}/\text{cm}^2$ )	FF
60	740	17.80	621.8	36.42	0.78
1	740	17.30	619.5	35.22	0.79
1	760	17.80	620.0	36.81	0.78
1	800	17.60	622.6	35.57	0.79

The highest efficiencies in this study are attributed to improvement in bulk lifetime after firing, as shown in Fig. 3. Average bulk lifetime increased to 80.4  $\mu\text{s}$  from 4.5  $\mu\text{s}$  with only 1 second firing. One second firing maintained bulk lifetime over 50  $\mu\text{s}$  even at 800 °C whereas bulk lifetime dropped rapidly at the temperatures above 740 °C for 60 second firing. This suggests that hydrogenation of bulk defects takes place in a very short time and the lifetime is determined by the release of hydrogen from the defects. The diffusivity of hydrogen is roughly estimated to be about  $9 \times 10^{-4} \text{ cm}^2/\text{s}$ , assuming that hydrogen diffuses through a 300  $\mu\text{m}$  thick wafer in 1 second at 740 °C. Van Weiregen and Warmoltz measured the hydrogen diffusivity in the temperature range of 1090 ~ 1200 °C [8].

$$D_H = 9.4 \times 10^{-3} \exp\left(\frac{-0.48 eV}{kT}\right) \text{ cm}^2 / \text{s} \quad (1)$$

Extrapolation of the diffusivity yields a diffusivity of  $3.846 \times 10^{-5} \text{ cm}^2/\text{s}$  at  $740 \text{ }^\circ\text{C}$ . In p-type Si, most of the hydrogen diffuses by rapid interstitial motion at high temperature over  $500 \text{ }^\circ\text{C}$  without any retardation by either acceptor trapping or molecule formation [9]. B.L.Sopori observed that hydrogen can diffuse through the entire wafer after 10 second annealing of  $\text{SiN}_x$  coated wafers at  $800^\circ\text{C}$  in an RTP chamber [10]. The much higher estimated diffusivity than the extrapolated value suggests that hydrogen diffusion may be enhanced by aluminum alloying induced vacancies [11].

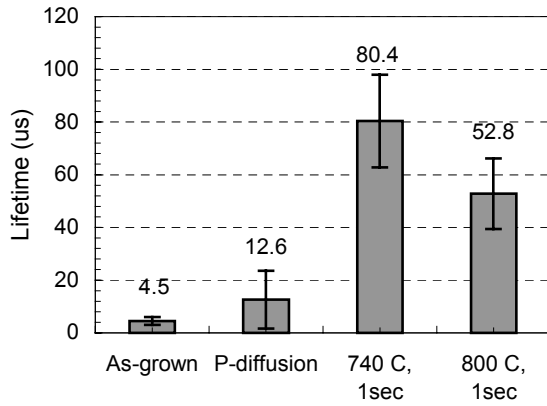


**Fig. 3** Effects of each process steps on the lifetime of String Ribbon.

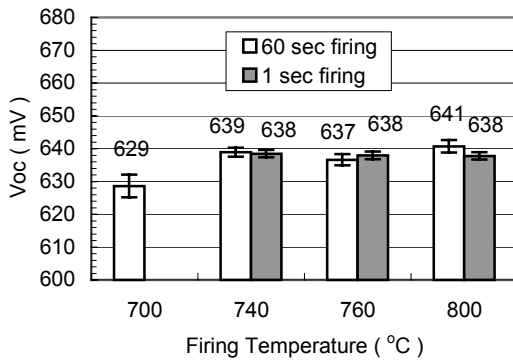


**Fig. 4**  $V_{oc}$  as a function of firing temperature and time. PL contact cells were fabricated on  $2 \text{ } \Omega\text{cm}$  FZ with rapid thermal oxide for emitter passivation and  $\text{ZnS/MgF}_2$  for antireflection coating.

In order to study the effects of firing temperature and time on the properties of the Al-BSF, photolithography cells were fabricated on  $2 \text{ } \Omega\text{cm}$  FZ wafers with rapid thermal oxide for emitter passivation. For all the firing conditions, the measured  $J_{oe}$  was  $2 \times 10^{-13} \text{ A/cm}^2$  without the metal contacts to the emitter. Therefore, the dependence of open circuit voltages on the firing temperature and time in Fig.4 were governed only by the Al-BSF quality. Note that the improvement in open circuit voltage saturated above firing temperatures of  $740 \text{ }^\circ\text{C}$ .

The IQE response of the cells in the range of  $750\text{-}1,000 \text{ nm}$  (Fig.5) indicates that the Al-BSF quality is not affected appreciably by the firing at temperatures over  $740 \text{ }^\circ\text{C}$  for both 1 and 60 second firing times.

The Al-BSF quality is determined by the junction depth, the doping concentration of the BSF layer, and the uniformity of the p-p<sup>+</sup> junction. The junction depth can be calculated from the Al-Si phase diagram using the following equation [12],

$$W_{BSF} = \frac{t_{Al} \cdot \rho_{Al}}{\rho_{Si}} \left( \frac{F(T)}{1 - F(T)} - \frac{F(T_o)}{1 - F(T_o)} \right) \quad (2)$$

where  $t_{Al}$ ,  $\rho_{Al}$  and  $\rho_{Si}$  represents the as-deposited Al thickness, the densities of Al and Si respectively,  $F(T)$  is the Si atomic weight percentage of the molten phase at the peak alloying temperature and  $F(T_o)$  is the Si atomic weight percentage at the eutectic temperature ( $\sim 12 \%$ ). The doping concentration of Al in the BSF is determined by the solid solubility of Al at each temperature as the BSF layer grows from the molten phase during the cooling cycle.

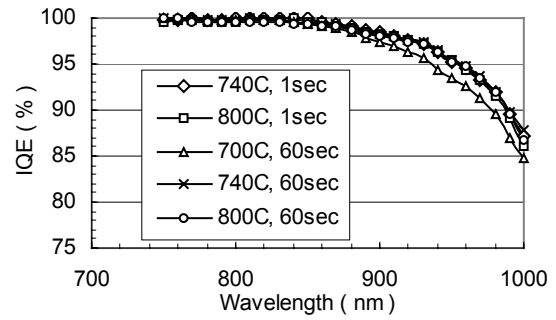


**Fig. 5** IQE responses for different firing processes.

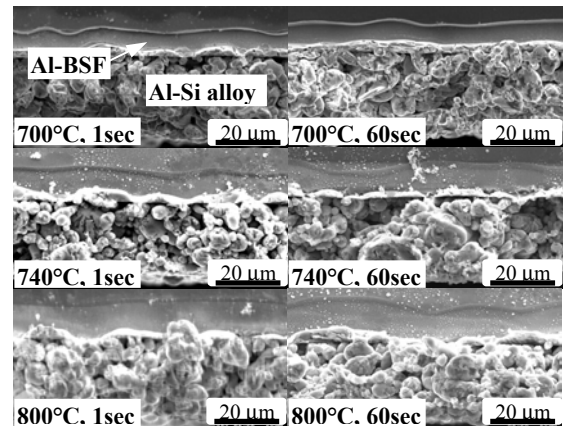


**Fig. 6** Cross-section SEM micrographs of the Al-BSF region for different firing processes.

Cross-section SEM images of the layers in the back were taken to measure uniformity and Al-BSF thicknesses after firing. Fig. 6 shows that uniform Al-BSF layers were observed for all the firing temperatures and times due to the high ramp-up rate. The Al-BSF thicknesses measured

from SEM images and calculated from equation 2 (ignoring the porosity of screen-printed Al) are shown in Fig. 7. The measured Al-BSF thickness was found to be greater than the calculated thickness using the Al-Si phase diagram at firing temperatures below 800 °C for firing times in the range of 1-60 second. The measured thicknesses tend to match calculated values at higher temperatures. For 1 second firing, the Al-BSF is thicker than the predicted value and exceeds 8 μm at temperatures over 740 °C. It is noteworthy that Al-Si alloying and 8 μm thick Si regrowth was accomplished in just a few seconds. It has been reported that the Al-BSF thickness corresponded to the calculated value at typical firing conditions (temperature range of 800-850 °C, time > 30 seconds). However, short time firing (1second) at low temperature (< 800 °C) is preferred for device performance as well as process speed, as shown earlier in this paper. The difference between the measured and calculated Al-BSF thickness from the theoretical value at lower temperatures suggests that thermodynamic equilibrium is not achieved or that the front and back surfaces of the wafers are at different temperatures during RTP firing.

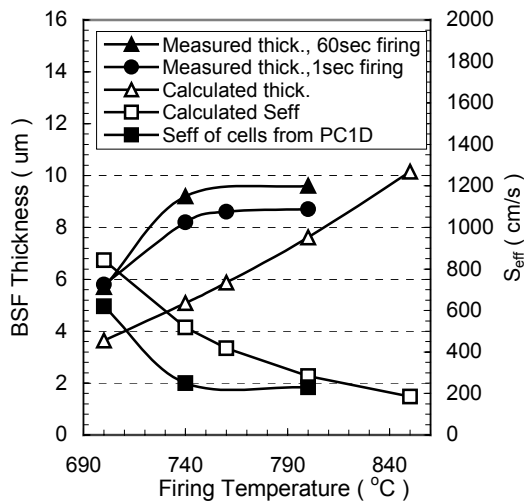


**Fig. 7** Al-BSF thicknesses and effective surface recombination velocities measured by SEM and calculated based on the Al-Si phase diagram.

## 5. CONCLUSIONS

We have successfully combined the industrial processing steps of SiN<sub>x</sub> AR coating and screen printed Al-BSF with the laboratory processes for double layer AR coating and photolithography contacts to produce record high 17.8 % efficient String Ribbon solar cells.

The bulk lifetime in String Ribbon improved significantly after phosphorus diffusion followed by firing of SiN<sub>x</sub> and Al in RTP. Only 1 second firing at 740 °C increased the bulk lifetime to 80 μs from 4.5 μs, suggesting that release of hydrogen from the defects is the limiting factor for maximum hydrogenation. About 8μm thick Al-BSF was formed with 1 second firing at temperatures greater than 740 °C and a ramp-up rate of over 50 °C/sec. SEM analysis confirmed that the measured

Al-BSF thickness was greater than the calculated thickness at firing temperatures lower than 800 °C, suggesting that thermodynamic equilibrium may not be achieved during short and rapid firing.

## REFERENCES

- [1] V.Yelundur, A.Rohatgi, J-W.Jeong, "PECVD SiN<sub>x</sub> induced hydrogen passivation in String Ribbon silicon", *Proceedings of the 28th Photovoltaic Specialists Conference*, (IEEE, Anchorage, 2000) p. 91.
- [2] J.I.Hanoka, "An overview of silicon ribbon growth technology", *Sol. Energy Mater. & Sol. Cells*, **65**, 231(2001).
- [3] G.Hahn, A.M.Gabor, "16% efficiency on encapsulated large area screen printed string ribbon cell", *The Third World Conference on Photovoltaic Energy Conversion*, (Osaka, 2003), in press.
- [4] V.Yelundur, A.Rohatgi, J.W.Jeong, J.Hanoka, "Improved String Ribbon silicon solar cell performance by rapid thermal firing of screen-printed contacts", *IEEE Tran. on Elec. Dev.*, **49**, no.8, 1405(2002).
- [5] V.Meemongkolkiat, M.Hilali, A.Rohatgi, "Investigation of RTP and belt fired screen printed Al-BSF on textured and planar back surfaces of silicon solar cells", *The Third World Conference on Photovoltaic Energy Conversion*, (Osaka, 2003), in press.
- [6] A.Rohatgi, V.Yelundur, J-W.Jeong, D.S.Kim, A.M.Gabor, "Implementation of rapid thermal processing to achieve greater than 15% efficient screen-printed ribbon silicon solar cells", *The Third World Conference on Photovoltaic Energy Conversion*, (Osaka, 2003), in press.
- [7] W.R. Runyan, *Semiconductor Measurements and Instrumentation* (McGraw-Hill: New York), 1975.
- [8] A.Van Wieringen and N.Warmoltz, *Physica* (Netherlands), **22**, 849(1956).
- [9] J.Pearson, W.Corbett and M.Stavola, *Hydrogen in crystalline semiconductors* (Springer-Verlag Heidelberg New York), 1991.
- [10] B.L.Sopori, Y.Zhang, and R.Reedy, "H diffusion for impurity and defect passivation: a physical model for solar cell processing", *Proceedings of the 29th Photovoltaic Specialists Conference(IEEE, New Orleans, 2002)*p.222.
- [11] J-W.Jeong, M.D.Rosenblum, J.P.Kalejs, and A.Rohatgi, "Hydrogenation of defects in edge-defined film-fed grown aluminum-enhanced plasma enhanced chemical vapor deposited silicon nitride multicrystalline silicon", *J. Appl. Phys.*, **87**, no.10, 7551(2000).
- [12] J.D. Alamo, J. Eguren, and A. Luque, "Operating limits of Al-alloyed high-low junctions for BSF solar cells", *Solid-State Electron.*, **24**, p. 415(1981).